PAPER • **OPEN ACCESS**

Effect of In and Cd co-doping on the thermoelectric properties of $Sn_{1-x}Pb_xTe$

To cite this article: Subhajit Roychowdhury and Kanishka Biswas 2019 *Mater. Res. Express* **6** 104010

Materials Research Express

PAPER

Effect of In and Cd co-doping on the thermoelectric properties of $Sn_{1-x}Pb_xTe$

Subhajit Roychowdhury[1] **and Kanishka Biswas**[1,2]

[1] New Chemistry Unit, Jawaharlal Nehru Centre for Advanced Scientific Research (JNCASR), Jakkur P O, Bangalore 560064, India
[2] School of Advanced Materials and International Centre of Materials Science, Jawaharlal Nehru Centre for Advanced Scientific Research (JNCASR), Jakkur P O, Bangalore 560064, India

E-mail: kanishka@jncasr.ac.in

Keywords: thermoelectric, SnTe, valence band convergence, resonant level

Supplementary material for this article is available online

OPEN ACCESS

RECEIVED
13 June 2019

REVISED
13 August 2019

ACCEPTED FOR PUBLICATION
22 August 2019

PUBLISHED
4 September 2019

Abstract

Pristine tin telluride (SnTe) with a similar electronic structure to PbTe shows inferior thermoelectric performance owing to high *p*-type hole concentration (10^{21} cm^{-3}), high lattice thermal conductivity, κ_{latt} (~2.8 W mK^{-1} at room temperature) and large energy gap between light and heavy hole valence bands. Interestingly, 30 mol% substitution of lead in SnTe decreases the excess hole carrier concentration and lattice thermal conductivity (~0.67 W $m^{-1}K^{-1}$ at 300 K) significantly. Here, we report the promising thermoelectric performance in $Sn_{0.70}Pb_{0.30}Te$ by enhancing the Seebeck coefficient via the co-adjuvant effect of resonant level formation and valence band convergence. We obtain a Seebeck coefficient value of ~141 μV K^{-1} at 300 K, which further increases to ~260 μV K^{-1} at 708 K for $Sn_{0.70}Pb_{0.30}Te$—3% Cd and 0.50% In sample. This is one of the highest *S* values for SnTe based system, to the best of our knowledge. In and Cd have discrete but complementary roles to augment the Seebeck coefficient value of $Sn_{0.70}Pb_{0.30}Te$ where In acts as a resonant dopant and Cd serves as valence band convergent, respectively, as demonstrated by the well-known Pisarenko plot of SnTe. Finally, we have achieved a maximum thermoelectric figure of merit, zT, of ~0.82 at 654 K for $Sn_{0.70}Pb_{0.30}Te$—3% Cd and 0.25% In sample.

Introduction

Thermoelectric (TE) technology has attracted attention recently as they are able to convert waste heat directly into electricity. The efficiency of TE materials is dependent upon the delicate concert of adversely interdependent parameters and is quantified in term of a dimensionless figure of merit (zT), defined as

$$zT = \frac{S^2\sigma}{\kappa_{el} + \kappa_{latt}}T$$

Where S is Seebeck coefficient, σ is electrical conductivity, κ_{el} is electrical thermal conductivity, κ_{latt} is lattice thermal conductivity and T is absolute temperature [1–9]. These three mutually interdependent parameters such as σ, S and κ_{el} provide hindrance in the pursuit of higher zT in a single material [1, 2]. The Last few decades have witnessed a significant enhancement of thermoelectric performance either by enhancing the Seebeck coefficient via manipulating the electronic band structure (band convergence or generation of the resonant level near Fermi level) [10–14] and/or reducing the thermal conductivity (lattice) by engineering phonon scattering sources [15–18].

PbTe is considered as an efficient thermoelectric material among IV–VI family for mid-temperature power generation applications [10, 13, 16]. However, pristine SnTe with a similar electronic structure to PbTe is not so popular as thermoelectric material because of its poor thermoelectric performance [5, 19]. This can be attributed to its high carrier concentration (10^{21} cm^{-3}), resulting from intrinsic Sn vacancy and large energy separation between light and heavy hole valence bands (~0.3–0.4 eV) than that of PbTe (~0.18 eV) which inhibit the

contribution of heavy hole valence band in the electrical transport and results low Seebeck coefficient [5, 16, 19–22]. Manipulation of electronic structure is an effective approach to improve the thermoelectric performance of SnTe by enhancing the Seebeck coefficient [5, 11, 12, 19, 23, 24]. Previously, Ren and coworkers revealed that indium (In) acts as a resonant dopant in SnTe and enhances the Seebeck coefficient significantly near room temperature [14]. Tan *et al* demonstrated that addition of Cd in SnTe decreases the energy gap between two valence bands and improves its Seebeck coefficient [23].

Moreover, pristine SnTe shows κ_{latt} of ~2.8 W $m^{-1}K^{-1}$ which is notably higher compare to its theoretical limit of minimum lattice thermal conductivity ($\kappa_{min} \sim 0.5$ W $m^{-1}K^{-1}$) at 300 K [18]. However, several approaches have been endeavored to reduce the κ_{latt} of SnTe based alloys to enhance the thermoelectric performance such as entropy engineering via introduction of multi principle element alloying [25], addition of nanoprecipitates of CdSe/HgTe [23, 26], encapsulation of layered intergrowth compound in matrix[18]. Recently, we have effectively reduced the κ_{latt} to ~0.67 W $m^{-1}K^{-1}$ in $Sn_{1-x}Ge_xTe$ by introducing the ferroelectric instability concept in the system without degrading the electrical transport [27]. In our previous work, we have shown that substitution of 30 mol% of Pb in SnTe effectively reduced the excess hole carrier concentration of SnTe and lattice thermal conductivity to ~0.67 W $m^{-1}K^{-1}$ at 300 K due to the enhanced solid solution point defect scattering [28]. Motivated by all these results, here, we thought to study the effect of co-substitution of In and Cd in $Sn_{0.70}Pb_{0.30}Te$ sample, which may improve the *S* values over a broad temperature range through the co-adjuvant effect of the resonance level formation and valence band convergence.

Herein, we demonstrate the promising thermoelectric performance of $Sn_{0.70}Pb_{0.30}Te$ sample by enhancing its Seebeck coefficient via the co-adjuvant effect of formation of the resonance level by In doping and valence band convergence enables by Cd doping. Co-doping of In and Cd increases the Seebeck coefficient of $Sn_{0.70}Pb_{0.30}Te$ sample significantly throughout the measured temperature range (300–710 K) compared to that of singly doped (In and Cd) $Sn_{0.70}Pb_{0.30}Te$ samples. We have attained a Seebeck coefficient value of ~141 μV K^{-1} at 300 K, which further increases to 260 μV K^{-1} at 708 K for $Sn_{0.70}Pb_{0.30}Te$—3% Cd and 0.50% In sample. As a result, a maximum zT of ~0.82 at 654 K for $Sn_{0.70}Pb_{0.30}Te$—3% Cd and 0.25% In sample which is higher compared to pristine SnTe and undoped $Sn_{0.70}Pb_{0.30}Te$ samples.

Results and discussion

The balance between the resonant level and valence band convergence is necessary to optimize the thermoelectric performance of the $Sn_{0.70}Pb_{0.30}Te$ system. Band convergence always requires relative high doping concentration to manipulate band dispersion in k-space [29]. In this work, we select Cd as the valence band convergent. The effect of band convergence will be stronger if the concentration of Cd is high [29]. Previous results confirm that the solubility of Cd is only 3 mol% in SnTe [23, 29]. Thus we fix the concentration of Cd is 3 mol% in the present work and then varies the concentration of resonant dopant, In. The resonant state is the deformation of the density of states (DOS) near Fermi level, and it reduces electrical conductivity significantly due to the reduction of carrier mobility at higher doping concentration [29]. Therefore, a lower concentration of resonant dopant and a higher concentration of band convergence dopant are always desired. Thus, the amount of In is varied from $x = 0$ to $x = 0.50$ mol%.

First, we have synthesized high quality crystalline ingots of $Sn_{0.70}Pb_{0.30}Te$—x % Cd and y % In ($x = 0$, $y = 0$; $x = 3$, $y = 0.05, 0.25, 0.50$) samples by vacuum sealed tube melting reaction (Details in methods, supporting information, SI). Powder x-ray diffraction (PXRD) patterns of $Sn_{0.70}Pb_{0.30}Te$—x % Cd and y % In ($x = 0, y = 0$; $x = 3, y = 0.05, 0.25, 0.50$) samples are presented in figures 1 and S1 available online at stacks.iop.org/MRX/6/104010/mmedia (zoomed version). The patterns confirm the formation of single-phase materials which crystallize in rock-salt structure (space group *Fm-3m*).

The temperature variations of electrical conductivity, σ, of $Sn_{0.70}Pb_{0.30}Te$—x % Cd and y % In ($x = 0$, $y = 0$; $x = 3$, $y = 0.05, 0.25, 0.50$) samples are shown in figure 2(a). The σ values for all the samples decrease with increasing temperature, like a degenerate semiconductor. Substitution of 3 mol% Cd reduces the σ from ~4260 S cm^{-1} for $Sn_{0.70}Pb_{0.30}Te$ to ~2500 S cm^{-1} for $Sn_{0.67}Cd_{0.03}Pb_{0.30}Te$ sample at 300 K (figures 2(a) and S2(a), SI). This confirms that the tendency of formation of Sn vacancy decreases with Cd substitution and reduces the hole carrier concentrations (table 1). Substitution of indium in $Sn_{0.70}Pb_{0.30}Te$—3% Cd sample further decreases the electrical conductivity owing to the significant reduction in carrier mobility due to resonant scattering, resulting from In doping (see table 1). Typically, σ of $Sn_{0.70}Pb_{0.30}Te$ sample is to be ~5471 S cm^{-1} at 300 K, which further decreases to ~ 620 S cm^{-1} at ~708 K. At room temperature, $Sn_{0.70}Pb_{0.30}Te$—3% Cd and 0.25% In sample exhibits a σ value of ~773 S cm^{-1} and reduces to ~264 S cm^{-1} at 708 K.

To determine the carrier concentration of $Sn_{0.70}Pb_{0.30}Te$—x % Cd and y% In ($x = 0, y = 0$; $x = 3$, $y = 0.05, 0.25, 0.50$) samples, Hall measurements were carried out (table 1). At room temperature, Hall

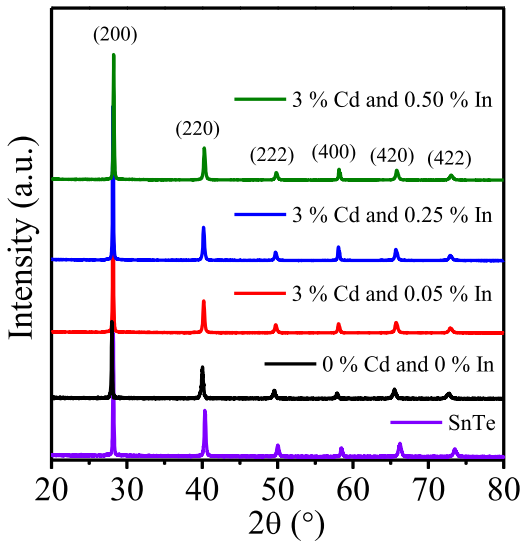

Figure 1. Powder XRD patterns of SnTe and $Sn_{0.70}Pb_{0.30}Te$—x % Cd and y % In (x = 0, y = 0; x = 3, y = 0.05, 0.25, 0.50) samples.

coefficients, R_H for all the samples are positive, indicating *p*-type conduction. Carrier concentration of undoped $Sn_{0.70}Pb_{0.30}Te$ sample is ~8 × 10^{19} cm^{-3}. Substitution of 3 mol% Cd decreases the carrier concentration of $Sn_{0.70}Pb_{0.30}Te$ sample due to the decreasing of Sn vacancies. The carrier concentration of $Sn_{0.70}Pb_{0.30}Te$—3% Cd and y % In samples decrease further with increasing In concentration (table 1). Notably, $Sn_{0.70}Pb_{0.30}Te$—3% Cd and y % In samples exhibit significantly low carrier mobility, resulting from resonant carrier scattering (table 1).

The temperature variations of Seebeck coefficient, *S*, of $Sn_{0.70}Pb_{0.30}Te$—x% Cd and y % In (x = 0, y = 0; x = 3, y = 0.05, 0.25, 0.50), controlled 3% Cd doped $Sn_{0.70}Pb_{0.30}Te$ and 0.25% In doped $Sn_{0.70}Pb_{0.30}Te$ samples are shown in figure 2(b) and S2(b), SI, respectively. Seebeck coefficient values for all the samples are positive which are consistent with our Hall coefficient data. Interestingly, for In and Cd co-doped $Sn_{0.70}Pb_{0.30}Te$ samples exhibit higher Seebeck coefficient value throughout the measured temperature range (300–710 K) compared to that of controlled In or Cd single doped $Sn_{0.70}Pb_{0.30}Te$ samples (figure S2(b), SI). Typically, the Seebeck coefficient value of $Sn_{0.70}Pb_{0.30}Te$—3% Cd and 0.50% In sample is ~140 $\mu V\ K^{-1}$ at 300 K and further increases to ~260 $\mu V\ K^{-1}$ at 708 K (figures 2(b), S3, SI). Thus, the synergistic effect of In and Cd co-doping in $Sn_{0.70}Pb_{0.30}Te$ is responsible for the observed notable augmentation in the Seebeck coefficient. At room temperature, highest Seebeck coefficient value is achieved in the present $Sn_{0.70}Pb_{0.30}Te$—3% Cd and 0.50% In sample which is higher than that of state-of-art SnTe based materials, to the best of our awareness [11, 12, 23–29, 31, 32].

To gain further insight into the origin of high Seebeck coefficient, we have plotted S values of $Sn_{0.70}Pb_{0.30}Te$—x% Cd and y % In (x = 0, y = 0; x = 3, y = 0.05, 0.25, 0.50) samples as a function of *p* and compared with the renowned Pisarenko line of SnTe (figure 2(c)) at 300 K [14]. Controlled In doped sample exhibits higher S value compared to theoretical Pisarenko line due to the formation of resonance level near the valence band of $Sn_{0.70}Pb_{0.30}Te$ similar to previously reported In doped SnTe and In doped $Sn_{0.70}Pb_{0.30}Te$ sample [14, 28]. Controlled Cd doped $Sn_{0.70}Pb_{0.30}Te$ sample shows a slightly higher Seebeck value compared to Pisarenko line, which is attributed to the effective valence band convergence. Interestingly, Cd and In co-doped $Sn_{0.70}Pb_{0.30}Te$ samples show remarkably higher Seebeck coefficient compared to that of singly doped (In and Cd) $Sn_{0.70}Pb_{0.30}Te$ samples. This confirms that In and Cd have distinct but complementary role to enhance the Seebeck coefficient, where In forms resonant level near valence band and Cd enables valence band convergence synergistically.

The temperature variations of power factor, $S^2\sigma$, of $Sn_{0.70}Pb_{0.30}Te$—x % Cd and y % In (x = 0, y = 0; x = 3, y = 0.05, 0.25, 0.50) samples are shown in figure 2(d). Typically, the $Sn_{0.70}Pb_{0.30}Te$—3% Cd and 0.25% In sample exhibits an $S^2\sigma$ value of ~9.8 $\mu Wcm^{-1}\ K^{-2}$ at 300 K, which increases further to ~ 15.9 $\mu Wcm^{-1}\ K^{-2}$ at 654 K. Co-substitution of In and Cd increases the Seebeck value in $Sn_{0.70}Pb_{0.30}Te$ but no improvement in $S^2\sigma$ value is observed owing to the significant decrease in electrical conductivity and mobility.

The temperature variations of total thermal conductivity, κ_{total}, of $Sn_{0.70}Pb_{0.30}Te$—x% Cd and y % In (x = 0, y = 0; x = 3, y = 0.05, 0.25, 0.50) samples are shown in figure 3(a). Co-substitution of In and Cd decreases the κ_{total} value of $Sn_{0.70}Pb_{0.30}Te$ sample. At 300 K, κ_{total} value reduces from 4.62 W $m^{-1}K^{-1}$ for $Sn_{0.70}Pb_{0.30}Te$ to 1.54 W $m^{-1}K^{-1}$ for $Sn_{0.70}Pb_{0.30}Te$—3% Cd and 0.25% In sample.

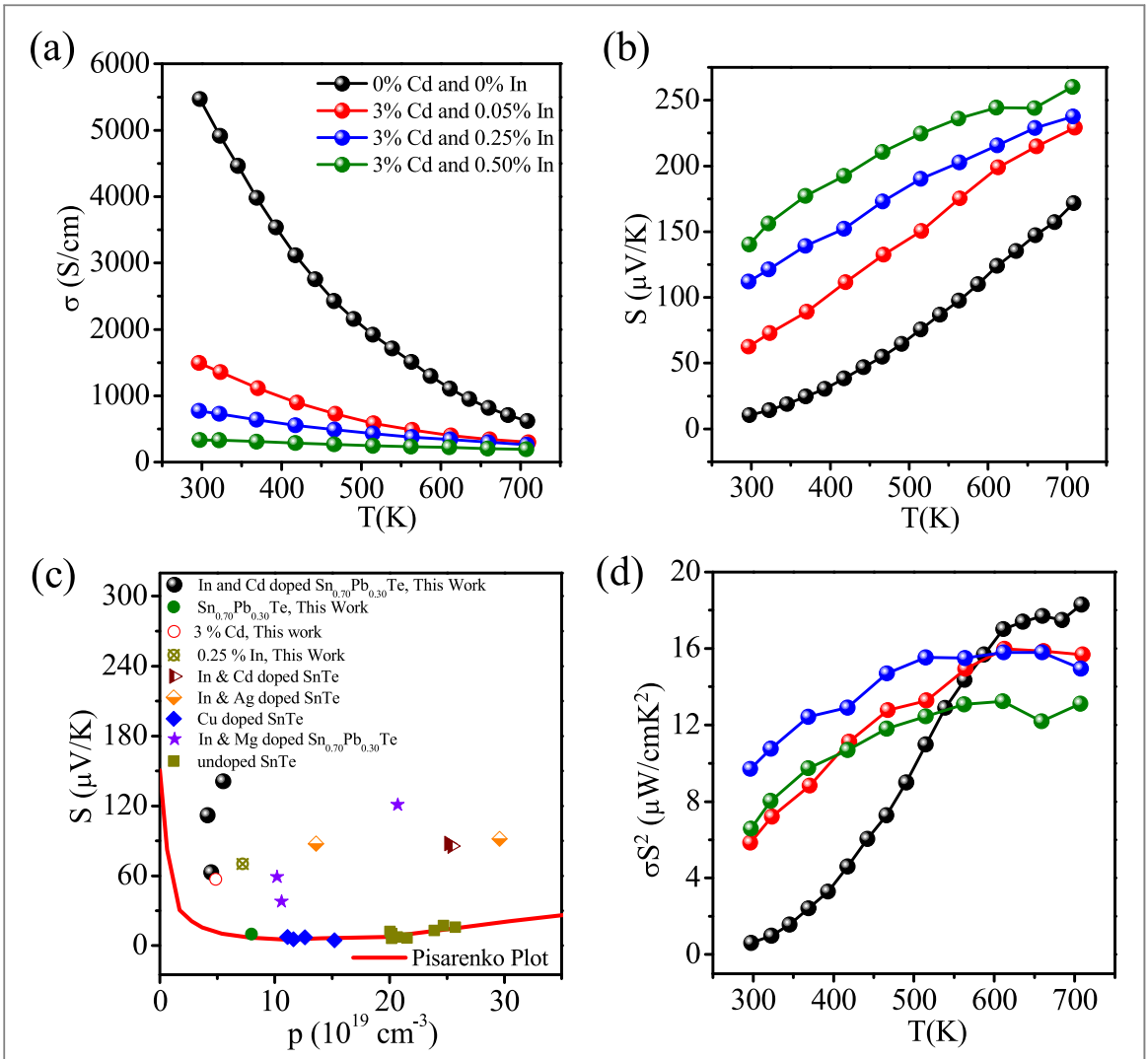

Figure 2. Temperature variations of (a) electrical conductivity (σ) and (b) Seebeck coefficient (S) of $Sn_{0.70}Pb_{0.30}Te$—x% Cd and y% In (x = 0, y = 0; x = 3, y = 0.05, 0.25, 0.50) samples. (c) Seebeck coefficient (S) of $Sn_{0.70}Pb_{0.30}Te$—x% Cd and y % In samples as a function of carrier concentration (p) at room temperature. For comparison, experimental data of un-doped $Sn_{0.70}Pb_{0.30}Te$ (present work), controlled Cd doped and In doped $Sn_{0.70}Pb_{0.30}Te$ (present work), previously reported In-Cd codoped SnTe [24], In-Ag codoped SnTe [11], In-Mg codoped $Sn_{0.70}Pb_{0.30}Te$ [28], undoped and Cu doped SnTe are presented in (c) [14, 30]. (d) Temperature variations of power factor (σS^2) of $Sn_{0.70}Pb_{0.30}Te$—x % Cd and y % In (x = 0, y = 0; x = 3, y = 0.05, 0.25, 0.50) samples.

Table 1. Room temperature carrier concentration (p) and mobility (μ) of $Sn_{0.70}Pb_{0.30}Te$—x % Cd and y % In (x = 0, y = 0; x = 3, y = 0.05, 0.25, 0.50), $Sn_{0.70}Pb_{0.30}Te$—3% Cd and $Sn_{0.70}Pb_{0.30}Te$—0.25% In samples.

Samples	p (10^{19} cm^{-3})	μ (cm^2 V^{-1}s^{-1})
$Sn_{0.70}Pb_{0.30}Te$	8	333
$Sn_{0.70}Pb_{0.30}Te$—3% Cd and 0.05% In	4.47	209
$Sn_{0.70}Pb_{0.30}Te$—3% Cd and 0.25% In	4.16	116
$Sn_{0.70}Pb_{0.30}Te$—3% Cd and 0.50% In	5.53	38
$Sn_{0.70}Pb_{0.30}Te$—3% Cd	4.86	321
$Sn_{0.70}Pb_{0.30}Te$—0.25% In	7.2	122

The noteworthy reduction in κ_{total} can be ascribed to the decrease in electrical thermal conductivity (κ_{el}) (figure 3(b)). The κ_{el} values for $Sn_{0.70}Pb_{0.30}Te$—3% Cd and y % In (y = 0.05, 0.25 and 0.50) samples are significantly lower compared to that of undoped $Sn_{0.70}Pb_{0.30}Te$, which is due to the considerably lower electrical conductivity for co-doped samples than that of undoped $Sn_{0.70}Pb_{0.30}Te$ sample (figure 2(a)). The κ_{el} values were calculated by using Wiedemann–Franz relation, $\kappa_{el} = L\sigma T$, where σ is measured electrical conductivity and L is calculated Lorenz number from reduced Fermi energy, which is acquired from the fitting of the temperature dependent S value [11, 12]. Typically, $Sn_{0.70}Pb_{0.30}Te$—3% Cd and 0.25% In sample exhibits κ_{el} value of ~0.43 W m^{-1}K^{-1} at 300 K and further reduces to ~0.30 W m^{-1}K^{-1} at 708 K. The lattice thermal conductivity,

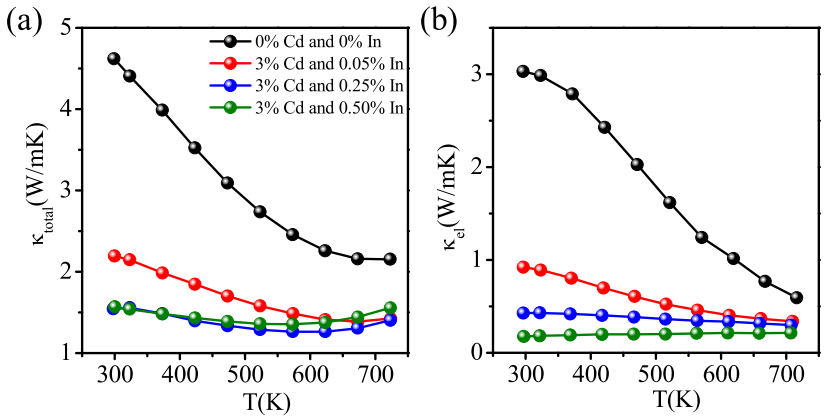

Figure 3. Temperature variations of (a) total thermal conductivity (κ_{total}) and (b) electrical thermal conductivity (κ_{el}) of $Sn_{0.70}Pb_{0.30}Te$—x% Cd and y% In (x = 0, y = 0; x = 3, y = 0.05, 0.25, 0.50) samples.

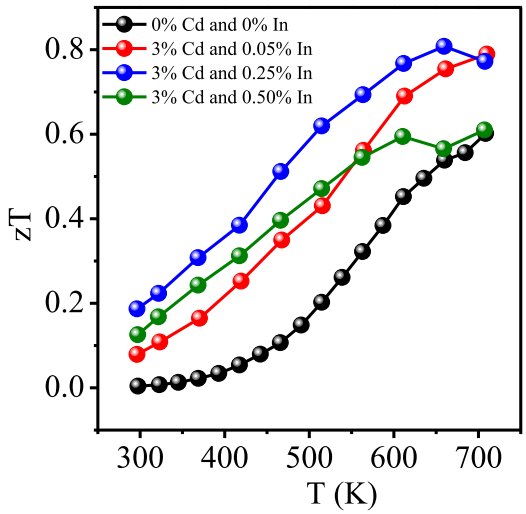

Figure 4. Temperature variations of thermoelectric figure of merit (zT) of $Sn_{0.70}Pb_{0.30}Te$—x% Cd and y % In (x = 0, y = 0; x = 3, y = 0.05, 0.25, 0.50) samples.

κ_{latt} was estimated after subtraction of electronic contribution from total thermal conductivity. $Sn_{0.70}Pb_{0.30}Te$—3% Cd and 0.25% In sample shows κ_{latt} value of 1.12 W $m^{-1}K^{-1}$ at 300 K and decreases to 1.06 W $m^{-1}K^{-1}$ at 708 K (figure S3, SI). Mention must be made that κ_{latt} values for $Sn_{0.70}Pb_{0.30}Te$—3% Cd and y% In (y = 0.05, 0.25 and 0.50) samples do not follow any systematic trend with dopant concentration which is similar with previously reported Ag-In co-doped SnTe and In-Mg co-doped $Sn_{0.70}Pb_{0.30}Te$ samples [11, 28].

The temperature variations of thermoelectric figure of merit, zT, of $Sn_{0.70}Pb_{0.30}Te$—x % Cd and y % In (x = 0, y = 0; x = 3, y = 0.05, 0.25, 0.50) samples are shown in figure 4. $Sn_{0.70}Pb_{0.30}Te$—3% Cd and 0.25% In sample exhibits the highest zT of ~0.82 at 654 K which is higher than undoped controlled $Sn_{0.70}Pb_{0.30}Te$ sample (~0.60 at 708 K).

Conclusions

We have prepared crystalline ingots of In and Cd codoped $Sn_{0.70}Pb_{0.30}Te$ samples via vacuum-sealed tube melting reaction. $Sn_{0.70}Pb_{0.30}Te$ sample exhibits κ_{latt} of ~0.67 W $m^{-1}K^{-1}$ at 300 which is close to the κ_{min} of SnTe (~0.50 W $m^{-1}K^{-1}$) due to the enhanced solid solution point defect scattering. Co-substitution of In and Cd increases the Seebeck coefficient of $Sn_{0.70}Pb_{0.30}Te$ sample significantly over a wide range of temperatures (300–710 K) compared to that of singly doped (In and Cd) $Sn_{0.70}Pb_{0.30}Te$ samples due to the co-adjuvant effect of resonance level formation near Fermi level and effective valence band convergence. At room temperature, highest Seebeck coefficient value has been realized in the present $Sn_{0.70}Pb_{0.30}Te$—3% Cd and 0.50% In sample (~141 μV K^{-1}) which is higher compared to that of state-of-the-art SnTe based materials. A maximum zT of

~0.82 is observed for $Sn_{0.70}Pb_{0.30}Te$—3% Cd and 0.25% In sample at 654 K which is higher than that of pristine SnTe and controlled $Sn_{0.70}Pb_{0.30}Te$ samples. Thermoelectric performance of $Sn_{0.70}Pb_{0.30}Te$ sample can be further improved by engineering phonon scattering centers via nanostructuring or all-scale hierarchical architecture.

Acknowledgments

This work was partially supported by DST-BRICS/KB/4567 and Sheikh Saqr Laboratory, JNCASR. SR thanks CSIR for fellowship.

ORCID iDs

Kanishka Biswas https://orcid.org/0000-0001-9119-2455

References

[1] Tan G, Zhao L D and Kanatzidis M G 2016 Rationally designing high-performance bulk thermoelectric materials *Chem. Rev.* **116** 12123
[2] Sootsman J, Chung D Y and Kanatzidis M G 2009 New and old concepts in thermoelectric materials *Angew. Chem. Int. Ed.* **48** 8616
[3] Ge Z H, Zhao L D, Wu D, Liu X, Zhang B P, Li J F and He J 2016 Low-cost, abundant binary sulfides as promising thermoelectric materials *Mater. Today* **19** 227
[4] Jana M K and Biswas K 2018 Crystalline solids with intrinsically low lattice thermal conductivity for thermoelectric energy conversion *ACS Energy Lett.* **3** 1315
[5] Banik A, Roychowdhury S and Biswas K 2018 The journey of tin chalcogenides towards high-performance thermoelectrics and topological materials *Chem. Commun.* **54** 6573
[6] Zhao L D, Dravid V P and Kanatzidis M G 2014 The panoscopic approach to high performance thermoelectrics *Energy Environ. Sci.* **7** 251
[7] Roychowdhury S, Samanta M, Perumal S and Biswas K 2018 Germanium chalcogenide thermoelectrics: electronic structure modulation and low lattice thermal conductivity *Chem. Mater.* **30** 5799
[8] Chandra S and Biswas K 2019 Realization of high thermoelectric figure of merit in solution synthesized 2D SnSe nanoplates via Ge alloying *J. Am. Chem. Soc.* **141** 6141
[9] Kim H S, Liu W, Chen G, Chu C W and Ren Z 2015 Relationship between thermoelectric figure of merit and energy conversion efficiency *Proc. Natl Acad. Sci. USA* **112** 8205
[10] Pei Y, Shi X, LaLonde A, Wang H, Chen L and Snyder G J 2011 Convergence of electronic bands for high performance bulk thermoelectrics *Nature* **473** 66
[11] Banik A, Shenoy U S, Saha S, Waghmare U V and Biswas K 2016 High power factor and enhanced thermoelectric performance of SnTe-$AgInTe_2$: synergistic effect of resonance level and valence band convergence *J. Am. Chem. Soc.* **138** 13068
[12] Banik A, Shenoy U S, Anand S, Waghmare U V and Biswas K 2015 Mg alloying in SnTe facilitates valence band convergence and optimizes thermoelectric properties *Chem. Mater.* **27** 581
[13] Heremans J P, Jovovic V, Toberer E S, Saramat A, Kurosaki K, Charoenphakdee A, Yamanaka S and Snyder G J 2008 Enhancement of thermoelectric efficiency in PbTe by distortion of the electronic density of states *Science* **321** 554
[14] Zhang Q, Liao B, Lan Y, Lukas K, Liu W, Esfarjani K, Opeil C, Broido D, Chen G and Ren Z 2013 High thermoelectric performance by resonant dopant indium in nanostructured SnTe *Proc. Natl Acad. Sci. USA* **110** 13261
[15] Chang C *et al* 2018 3D charge and 2D phonon transports leading to high out-of-plane ZT in n-type SnSe crystals *Science* **360** 778
[16] Biswas K, He J, Blum I D, Wu C I, Hogan T P, Seidman D N, Dravid V P and Kanatzidis M G 2012 High-performance bulk thermoelectrics with All-scale hierarchical architectures *Nature* **489** 414
[17] Poudel B *et al* 2008 High-thermoelectric performance of nanostructured bismuth antimony telluride bulk alloys *Science* **320** 634
[18] Banik A, Vishal B, Perumal S, Datta R and Biswas K 2016 The origin of low thermal conductivity in $Sn_{1-x}Sb_xTe$: phonon scattering via layered intergrowth nanostructures *Energy Environ. Sci.* **9** 2011
[19] Li W, Wu Y, Lin S, Chen Z, Li J, Zhang X, Zheng L and Pei Y 2017 Advances in environment friendly SnTe thermoelectrics *ACS Energy Lett.* **2** 2349
[20] Brebrick R and Strauss A 1963 Anomalous thermoelectric power as evidence for two-valence bands in SnTe *Phys. Rev.* **131** 104
[21] Rogers L M 1968 Valence band structure of SnTe *J. Phys. D: Appl. Phys.* **1** 845
[22] Rogacheva E I 2008 The problem of doping of non-stoichiometric phases *J. Phys. Chem. Solids* **69** 259
[23] Tan G, Zhao L D, Shi F, Doak J W, Lo S H, Sun H, Wolverton C, Dravid V P, Uher C and Kanatzidis M G 2014 High thermoelectric performance of p-Type SnTe via a synergistic band engineering and nanostructuring approach *J. Am. Chem. Soc.* **136** 7006
[24] Tan G, Shi F, Hao S, Chi H, Zhao L D, Uher C, Wolverton C, Dravid V P and Kanatzidis M G 2015 Codoping in SnTe: enhancement of thermoelectric performance through synergy of resonance levels and band convergence *J. Am. Chem. Soc.* **137** 5100
[25] Hu L, Zhang Y, Wu H, Li J, Li Y, Mckenna M, He J, Liu F, Pennycook S J and Zeng X 2018 Entropy engineering of SnTe: multi-principal-element alloying leading to ultralow lattice thermal conductivity and state-of-the-Art thermoelectric performance *Adv. Energy Mater.* **8** 1802116
[26] Tan G, Shi F, Doak J W, Sun H, Zhao L D, Wang P L, Uher C, Wolverton C, Dravid V P and Kanatzidis M G 2015 Extraordinary role of Hg in enhancing the thermoelectric performance of p-type SnTe *Energy Environ. Sci.* **8** 267
[27] Banik A, Ghosh T, Arora R, Dutta M, Pandey J, Acharya S, Soni A, Waghmare U V and Biswas K 2019 Engineering ferroelectric instability to achieve ultralow thermal conductivity and high thermoelectric performance in $Sn_{1-x}Ge_xTe$ *Energy Environ. Sci.* **12** 589
[28] Roychowdhury S, Shenoy U S, Waghmare U V and Biswas K 2017 An enhanced Seebeck coefficient and high thermoelectric performance in p-type In and Mg co-doped $Sn_{1-x}Pb_xTe$ via the co-adjuvant effect of the resonance level and heavy hole valence band *J. Mater. Chem. C* **5** 5737

[29] Tan X, Tan X, Liu G, Xu J, Shao H, Hu H, Jin M, Jiang H and Jiang J 2017 Optimizing the thermoelectric performance of In–Cd codoped SnTe by introducing Sn vacancies *J. Mater. Chem. C* **5** 7504
[30] Brebrick R F and Strauss A J 1963 Anomalous thermoelectric power as evidence for two valence bands in SnTe *Phys. Rev.* **131** 104
[31] Tan G, Shi F, Hao S, Chi H, Bailey T P, Zhao L D, Uher C, Wolverton C, Dravid V P and Kanatzidis M G 2015 Valence band modification and high thermoelectric performance in SnTe heavily alloyed with MnTe *J. Am. Chem. Soc.* **137** 11507
[32] Wang L, Tan X, Liu G, Xu J, Shao H, Yu B, Jiang H, Yue S and Jiang J 2017 Manipulating band convergence and resonant state in thermoelectric material SnTe by Mn—In codoping *ACS Energy Lett.* **2** 1203